RSC Advances

PAPER

View Article Online
View Journal | View Issue

Cite this: *RSC Adv.*, 2022, **12**, 25687

Fluorescent polymer films based on photo-induced electron transfer for visualizing water†

Saori Miho, Keiichi Imato * and Yousuke Ooyama *

As fluorescent materials for visualization, detection, and quantification of a trace amount of water, we have designed and developed a PET (photo-induced electron transfer)-type fluorescent monomer **SM-2** composed of methyl methacrylate-substituted anthracene fluorophore-(aminomethyl)-4-cyanophenylboronic acid pinacol ester (AminoMeCNPhenylBPin) and achieved preparation of a copolymer **poly(SM-2-*co*-MMA)** composed of **SM-2** and methyl methacrylate (MMA). Both **SM-2** and **poly(SM-2-*co*-MMA)** exhibited enhancement of the fluorescence emission with the increase in water content in various solvents (less polar, polar, protic, and aprotic solvents) due to the formation of the PET inactive (fluorescent) species **SM-2a** and **poly(SM-2-*co*-MMA)a**, respectively, by the interaction with water molecules. The detection limit (DL) of **poly(SM-2-*co*-MMA)** for water in the low water content region below 1.0 wt% in acetonitrile was 0.066 wt%, indicating that **poly(SM-2-*co*-MMA)** can act as a PET-type fluorescent polymeric sensor for a trace amount of water in solvents, although it was inferior to that (0.009 wt%) of **SM-2**. It was found that spin-coated **poly(SM-2-*co*-MMA)** films as well as 15 wt% **SM-2**-doped polymethyl methacrylate (PMMA) films produced a satisfactory reversible fluorescence off–on switching between the PET active state under a drying process and the PET inactive state upon exposure to moisture, which is demonstrated by the fact that the both the films are similar in hydrophilicity to each other from the measurement of the water contact angles on the polymer film surface. Herein we propose that PET-type fluorescent polymer films based on a fluorescence enhancement system are one of the most promising and convenient functional dye materials for visualizing moisture and water droplets.

Received 24th June 2022
Accepted 2nd September 2022

DOI: 10.1039/d2ra03894c

rsc.li/rsc-advances

Introduction

In recent years, concern has been raised about the development of fluorescent sensors and their functional materials such as polymer films and sensor-immobilized membranes for visualizing water in solutions, solids, and gas or on material surfaces, from the viewpoint of their potential applications to environmental and quality control monitoring systems and industry, as well as fundamental study in photochemistry, analytical chemistry, and photophysics.[1–23] Several investigations have been conducted on the design and synthesis of organic fluorescent sensors and polymers for the detection of water based on ICT (intramolecular charge transfer),[24–34] ESIPT (excited state intramolecular proton transfer),[35–38] PET (photo-induced electron transfer),[39–46] or solvatochromism[47–52] and the elucidation of the optical sensing properties based on changes in wavelength, intensity, and lifetime of fluorescence emission depending on the water content. It was demonstrated that most of ICT- and ESIP-type fluorescent sensors and fluorescent conjugated polymers exhibited attenuation of the fluorescence emission, that is, fluorescence quenching (turn-off) systems with the increase in water content in solvents, and were suitable for the detection and quantification of a trace amount of water (below 1–10 wt% in almost every case) in solvents. However, one can see that the fluorescence quenching (turn-off) systems make it difficult to visually confirm the presence of water in samples and on material surfaces. On the other hand, the PET-type fluorescent sensors are based on a fluorescence enhancement (turn-on) system and showed the increase in the fluorescence intensity with the increase in water content in solvents, so that it allowed us to visually confirm the presence of water in samples and on material surfaces. Thus, we have focused on the design and development of PET-type fluorescent sensors for the detection and quantification of water and the preparation of their functional materials for visualizing water. In our continuous work for the improvement of the sensitivity and accuracy of PET-type fluorescent sensors for water during the past decade, we have demonstrated that anthracene-(aminomethyl)-4-cyanophenylboronic acid pinacol ester (AminoMeCNPhenylBPin) **OF-2** and its derivative **SM-1** having a hydroxymethyl group on the anthracene skeleton were highly

Applied Chemistry Program, Graduate School of Advanced Science and Engineering, Hiroshima University, 1-4-1 Kagamiyama, Higashi-Hiroshima 739-8527, Japan. E-mail: yooyama@hiroshima-u.ac.jp

† Electronic supplementary information (ESI) available. See https://doi.org/10.1039/d2ra03894c

sensitive PET-type fluorescence sensors for the detection and quantification of a trace amount of water in polar, less polar, protic, and aprotic solvents (Fig. 1a and b).[23,42] In each sensor, the PET takes place from the nitrogen atom of the amino moiety to the photoexcited anthracene fluorophore in the absence of water, leading to quenching of the fluorescence. When water was added to the solution of **OF-2** or **SM-1**, the nitrogen atom of the amino moiety was protonated or strongly interacted with water molecules to form the PET inactive (fluorescent) species **OF-2a** or **SM-1a**, and as a result, a drastic enhancement of the fluorescence emission was observed due to the suppression of PET. Indeed, the detection limits (DLs) and quantitation limits (QLs) of **OF-2** and **SM-1** for water in acetonitrile were, respectively, 0.009 wt% and 0.026 wt% and 0.004 wt% and 0.013 wt%, which were equivalent or superior to those of the fluorescence quenching systems (turn-off) based on the reported ICT-type[24–34] and ESIPT-type[35–38] fluorescent sensors. Thus, the PET method based on the fluorescence enhancement (turn-on) system makes it possible to visualize, detect, and determine a trace amount of water in solvents.

Meanwhile, under the Coronavirus Disease 2019 (COVID-19) situation, face shields made of polyester or polycarbonate films and partitions made of acrylic resin are one of convenience and commercially available protective goods for reducing the risk of droplet infection. Therefore, if we can visually confirm the presence of droplets containing infectious viruses on the face shields and partitions, this allows us to accurately remove the viruses by wiping away the droplets. However, the virus-containing droplets are generally 5 μm or more which is too small for our eyes to see. Nevertheless, because over 90% of the droplets is composed of water, functional materials as well as techniques and methods capable of visualizing water are undoubtedly useful for detecting the virus-containing droplets. In our previous work, for this purpose, we have achieved the preparation of various types of fluorescent polymer films (polystyrene, poly(4-vinylphenol), polyvinyl alcohol, and polyethylene glycol) doped with the PET-type fluorescent sensor **OF-2** or **SM-1**.[22,23] It was found that the **OF-2**- or **SM-1**-doped polymer films exhibited a reversible switching of the fluorescent color between feeble green excimer emission in the PET active state under a drying process and intense blue monomer emission in the PET inactive state upon exposure to moisture or water droplets. Our previous work is the first to achieve the preparation of PET-type fluorescent sensor-doped polymer films for water, while ICT-type[32–34] or ESIPT-type[37,38] fluorescent sensor-doped polymer films and fluorescent conjugated polymers[18–21,53,54] for water based on a fluorescence quenching (turn-off) system have been reported. However, the reversibility of the fluorescence intensity of **OF-2**- or **SM-1**-doped polymer films between the excimer and monomer emissions in the dry–wet process were not fully satisfactory for the practical use for the visualization and detection of water on materials surfaces, due to destruction of the films during the dry–wet process.

Thus, in this work, to improve the reversibility of the fluorescence intensity of PET-type fluorescent polymer films by giving strong durability during the dry–wet process, we have designed and developed a PET-type fluorescent monomer **SM-2** having a methyl methacrylate group on the anthracene skeleton as a derivative of **SM-1** and achieved preparation of a copolymer **poly(SM-2-*co*-MMA)** composed of **SM-2** and methyl methacrylate (MMA) (Fig. 1c and d). It was found that spin-coated **poly(SM-2-*co*-MMA)** films as well as **SM-2**-doped polymethyl methacrylate (PMMA) films produced a satisfactory reversible fluorescence off–on switching between the PET active state under a drying process and the PET inactive state upon exposure to moisture, which is demonstrated by the fact that the both the films are similar in hydrophilicity to each other from the measurement of the water contact angles on the polymer film surface. Herein we propose that PET-type fluorescent polymer films based on a fluorescence enhancement system are one of the most promising and convenient functional dye materials for visualizing moisture and water droplets.

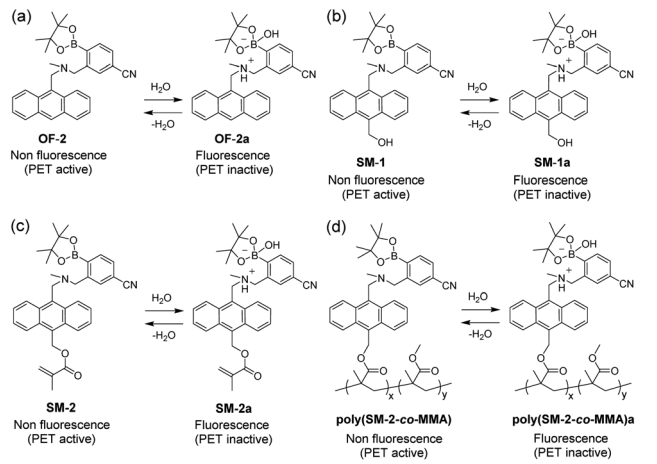

Fig. 1 Mechanisms of PET-type fluorescent sensors (a) OF-2, (b) SM-1 (previous work), (c) SM-2, and (d) poly(SM-2-*co*-MMA) (this work) for detection of water in organic solvents and films.

Results and discussion

The PET-type fluorescent monomer **SM-2** was prepared by the reaction of **SM-1**[23] with methacryloyl chloride (Scheme 1). Then, polymerization was carried out by a ratio of **SM-2** and MMA of 1 : 20 using 2,2′-azobis(isobutyronitrile) (AIBN)[55] as a free radical initiator to give **poly(SM-2-*co*-MMA)** as a white solid (M_n = 18 900, M_w/M_n = 2.08, 17% yield). As the result, the ^{1}H NMR spectrum indicated that the molar ratio (y/x) of MMA unit (y) and **SM-2** unit (x) and the weight percentage (wt%) of **SM-2** in

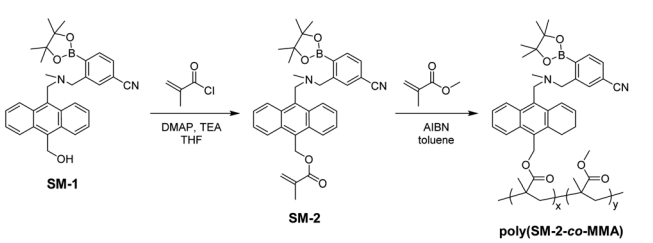

Scheme 1 Synthesis of SM-2 and poly(SM-2-*co*-MMA).

the obtained **poly(SM-2-*co*-MMA)** were determined to be *ca.* 40 and *ca.* 15 wt%, respectively.

The optical sensing ability of the PET-type fluorescent monomer **SM-2** for water in solvents was investigated by photoabsorption and fluorescence spectral measurements in 1,4-dioxane and THF as less polar solvents, acetonitrile as a polar solvent, and ethanol as a protic solvent containing various concentrations of water (in the water content region below 10 wt%) (Fig. 2). As with the cases of **OF-2**[42] and **SM-1**,[23] **SM-2** in all the four solvents showed a vibronically-structured photoabsorption band in the range of 300 nm to 400 nm originating from the anthracene skeleton and did not undergo appreciable changes in the absorbance and shape upon the addition of water to the solutions (Fig. 2a, c, e and g). For the corresponding fluorescence spectra, **SM-2** in the absolute solvents exhibited a feeble and vibronically-structured fluorescence band with a fluorescence maximum wavelength (λ^{fl}_{max}) at around 420 nm in the range of 400 nm to 500 nm, which is attributed to the monomer emission originating from the anthracene fluorophore in the PET active state (Fig. 2b, d, f and h). On the other hand, in the low water content region below 1.0 wt%, the fluorescence band increased in the intensity with the increase in the water content in the solution, which is attributed to the formation of the PET inactive (fluorescent) species **SM-2a** by the addition of a water molecule, as with the cases of **OF-2**[42] and **SM-1**[23] (Fig. 1a–c). As shown in Fig. 3a, the acetonitrile solution of **SM-2** without the addition of water did not show visual fluorescence emission but exhibited the blue fluorescence emission originating from the anthracene fluorophore upon the addition of water. In fact, to confirm the formation of the PET inactive species **SM-2a** by the interaction with a water molecule, we performed ^{1}H NMR spectral measurements of **SM-2** with and without the addition of water in the acetonitrile-d_3 solution (2.0×10^{-2} M) (Fig. 4). The ^{1}H NMR spectrum of the **SM-2** solution (water content of 0.49 wt%) without the addition of water showed an obvious signal that can be assigned to a single chemical species with the **SM-2** structure. On the other hand, some additional signals appeared in both the aliphatic and aromatic regions in the ^{1}H NMR spectrum of the **SM-2** solution with water content of 2.3 wt%, compared to that of the solution without the addition of water, indicating the existence of other chemical species as well as **SM-2**. Moreover, for the ^{1}H NMR spectrum of the **SM-2** solution with water content of 13 wt%, the chemical shifts of the methyl protons H_a of boronic acid pinacol ester, the aminomethyl protons H_c, and the aromatic protons H_n and H_o of the anthracene skeleton showed considerably upfield shifts, while those of the methylene protons H_e next to the anthracene skeleton and the aromatic protons H_i and H_k of the phenyl group showed considerably downfield shifts. Consequently, the

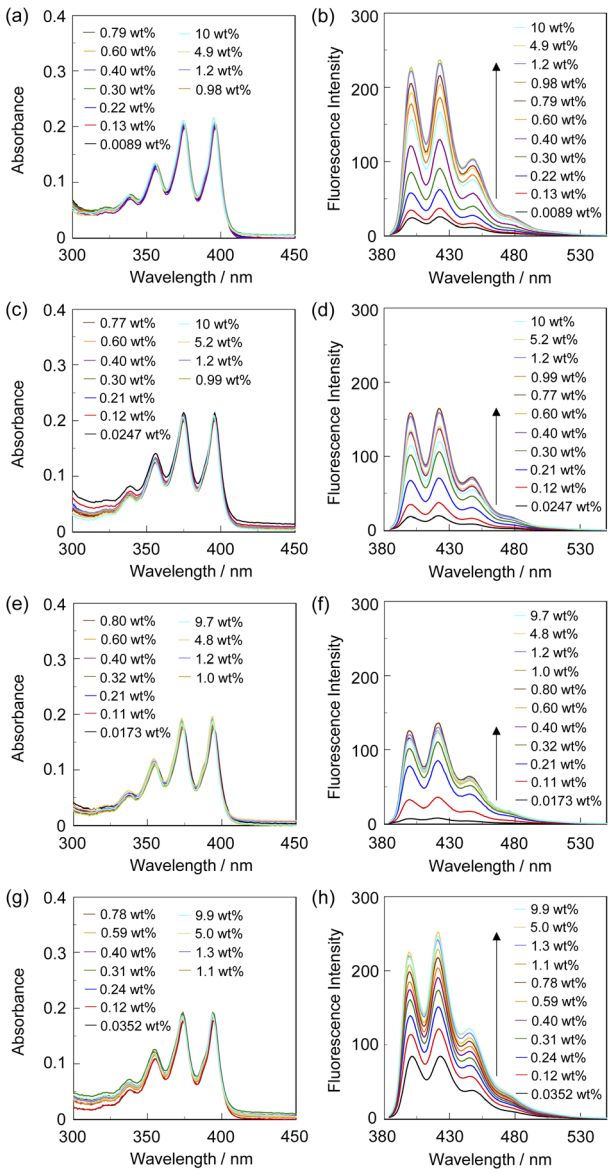

Fig. 2 (a) Photoabsorption and (b) fluorescence spectra ($\lambda^{ex} = 375$ nm) of **SM-2** (2.0×10^{-5} M) in 1,4-dioxane containing water (0.0089–10 wt%). (c) Photoabsorption and (d) fluorescence spectra ($\lambda^{ex} = 375$ nm) of **SM-2** (2.0×10^{-5} M) in THF containing water (0.0247–10 wt%). (e) Photoabsorption and (f) fluorescence spectra ($\lambda^{ex} = 374$ nm) of **SM-2** (2.0×10^{-5} M) in acetonitrile containing water (0.0173–9.7 wt%). (g) Photoabsorption and (h) fluorescence spectra ($\lambda^{ex} = 374$ nm) of **SM-2** (2.0×10^{-5} M) in ethanol containing water (0.0352–9.9 wt%).

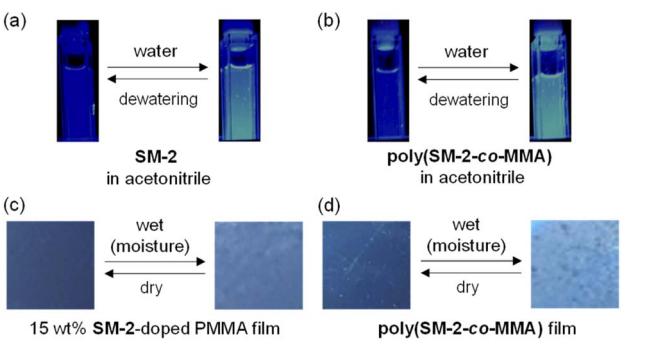

Fig. 3 Photographs (under 365 nm irradiation) of acetonitrile solutions of (a) **SM-2** and (b) **poly(SM-2-*co*-MMA)** before and after addition of water and (c) 15 wt% **SM-2**-doped PMMA film and (d) **poly(SM-2-*co*-MMA)** film before and after exposure to moisture.

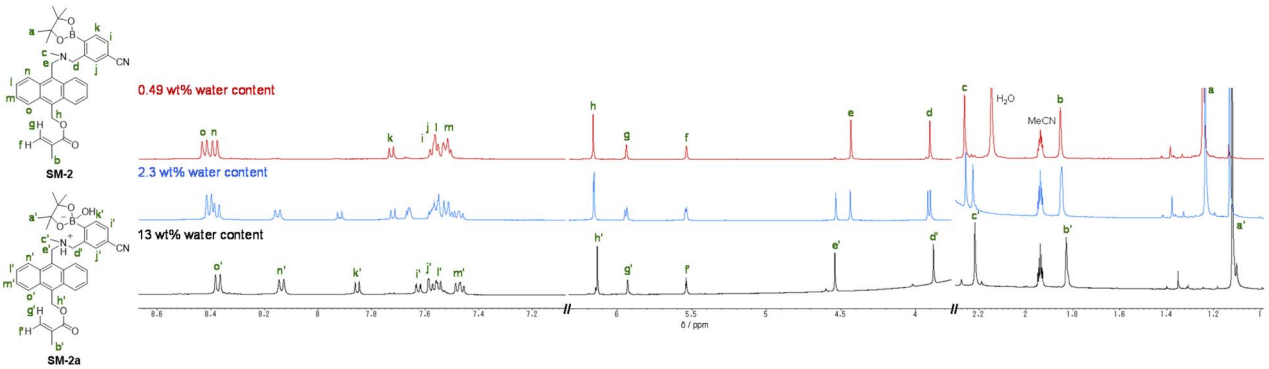

Fig. 4 ^{1}H NMR spectra of **SM-2** (2.0×10^{-2} M) in acetonitrile-d_3 with 0.49 wt%, 2.3 wt%, and 13 wt% water content.

fact strongly indicates that the PET inactive species **SM-2a** interacted with water molecules occurred upon the addition of water to the **SM-2** solution (Fig. 1c), as with the cases of **OF-2**[42] and **SM-1**.[23]

The sensitivity and accuracy of **SM-2** for the detection of water in solvents were evaluated by the changes in the fluorescence peak intensity at around 420 nm and the plots against the water fraction in solvents (Fig. 5). The plots for **SM-2** demonstrated that the fluorescence peak intensity increased linearly as a function of the water content in the low water content region below 1.0 wt% in all four solvents (Fig. 5a), while the fluorescence intensity leveled off when the water content reached 1.0 wt% as with the cases of **OF-2**[42] and **SM-1**.[23] The results of the plots for **SM-2** are as follows:

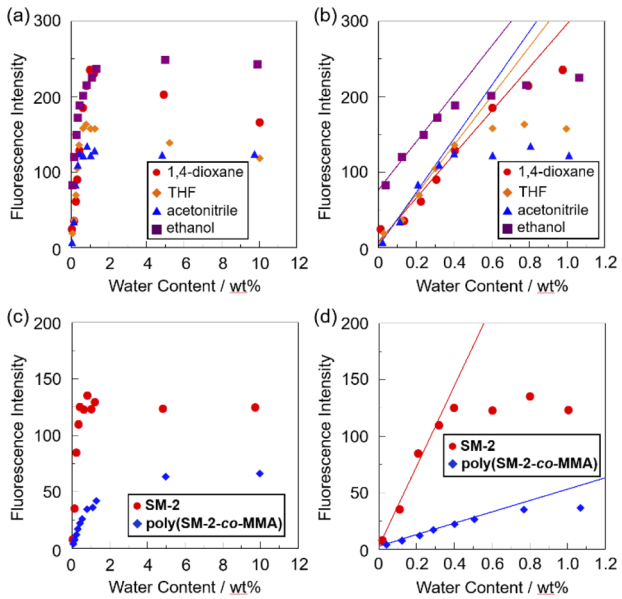

Fig. 5 Fluorescence peak intensity at around 420 nm of **SM-2** (λ^{ex} = 374 or 375 nm) as a function of water content below (a) 10 wt% and (b) 1.1 wt% in 1,4-dioxane, THF, acetonitrile, and ethanol. Fluorescence peak intensity at around 420 nm of **SM-2** (λ^{ex} = 374 nm) and **poly(SM-2-*co*-MMA)** (λ^{ex} = 375 nm) as a function of water content below (c) 10 wt% and (d) 1.1 wt% in acetonitrile.

$$\text{1,4-Dioxane: } F = 288.6[H_2O] + 7.99 \ (R^2 = 0.974, [H_2O] = 0.0089\text{–}0.60 \text{ wt\%}) \quad (1)$$

$$\text{THF: } F = 326.0[H_2O] + 5.32 \ (R^2 = 0.986, [H_2O] = 0.0247\text{–}0.40 \text{ wt\%}) \quad (2)$$

$$\text{Acetonitrile: } F = 355.5[H_2O] + 2.10 \ (R^2 = 0.977, [H_2O] = 0.0173\text{–}0.32 \text{ wt\%}) \quad (3)$$

$$\text{Ethanol: } F = 317.6[H_2O] + 76.7 \ (R^2 = 0.988, [H_2O] = 0.0352\text{–}0.31 \text{ wt\%}) \quad (4)$$

The correlation coefficient (R^2) values for the calibration curves of **SM-2** were 0.974–0.988, which indicates good linearity. A linear change in fluorescence intensity as a function of water content is one of the factors required for the practical use of a fluorescence sensor for water.[39–43] The intercept values (2.1–76.7) demonstrated that the plots for 1,4-dioxane, THF, and acetonitrile fit straight lines passing through almost the origin, which also indicates the fluorescence enhancement due to the formation of the PET inactive species **SM-2a** with the increase in the water content. Meanwhile, it is considered that the enhanced fluorescence of **SM-2** in absolute ethanol is attributed to the suppression of PET by the hydrogen bonding between the hydroxyl group of ethanol and the amino moiety of **SM-2**, as with the cases of **OF-2**[42] and **SM-1**.[23] It is worth mentioning here that there was a little difference in the m_s values (288–355) for **SM-2** between the four solvents, while the m_s values for **SM-2** were equivalent to those for **OF-2** but smaller than those for **SM-1** (Table 1). The large m_s values for **SM-1** relative to **SM-2** and **OF-2** can be attributed to the fact that the fluorescence emission property was improved by the introduction of a hydroxymethyl group to the anthracene fluorophore. Actually, fluorescence quantum yields (Φ_{fl}) of **OF-2**, **SM-1**, and **SM-2** in absolute acetonitrile were below 2%, but in acetonitrile with 1.0 wt% water content, the Φ_{fl} (20%) of **SM-1** was higher than those (13% and 12%, respectively) of **OF-2** and **SM-2**. The DLs and QLs of **SM-2** for water in the solvents were determined based on the following equations: DL = $3.3\sigma/m_s$ and QL = $10\sigma/m_s$, where σ is the standard deviation of blank sample and m_s is the slope of a calibration curve obtained from the plot of the fluorescence

Table 1 DLs and QLs of **OF-2**, **SM-1**, **SM-2**, and **poly(SM-2-*co*-MMA)** for water in various organic solvents

Sensor	Solvent	m_s[a]	DL[b]	QL[c]
OF-2[42]	1,4-Dioxane	334	0.01 wt%	0.03 wt%
	THF	390	0.008 wt%	0.026 wt%
	Acetonitrile	382	0.009 wt%	0.026 wt%
	Ethanol	362	0.009 wt%	0.027 wt%
SM-1[23]	1,4-Dioxane	564	0.006 wt%	0.018 wt%
	THF	819	0.004 wt%	0.012 wt%
	Acetonitrile	753	0.004 wt%	0.013 wt%
	Ethanol	484	0.007 wt%	0.021 wt%
SM-2	1,4-Dioxane	288	0.011 wt%	0.035 wt%
	THF	326	0.01 wt%	0.03 wt%
	Acetonitrile	355	0.009 wt%	0.028 wt%
	Ethanol	317	0.01 wt%	0.032 wt%
poly(SM-2-*co*-MMA)	Acetonitrile	50	0.066 wt%	0.2 wt%

[a] Slope of calibration curve. [b] Detection limit (DL) and quantitation limit (QL) of sensor for water. [c] Detection limit (DL) and quantitation limit (QL) of sensor for water.

peak intensity at around 420 nm the water fraction in the low water content region below 1.0 wt% (Fig. 5b). The DLs and QLs of **SM-2** for water were, respectively, 0.011 and 0.035 wt% in 1,4-dioxane, 0.01 and 0.03 wt% in THF, 0.009 and 0.028 wt% in acetonitrile, and 0.01 and 0.032 wt% in ethanol, which were equivalent to those of **OF-2** but inferior to those of **SM-1**. Consequently, it was found that methyl methacrylate-substituted anthracene-AminoMeCNPhenylBPin **SM-2** can act as a PET-type fluorescent sensor for the detection and quantification of a trace amount of water in polar, less polar, protic, and aprotic solvents, as with the reported PET-type fluorescent sensors for water including **OF-2** and **SM-1**.

To investigate the optical sensing ability of the copolymer **poly(SM-2-*co*-MMA)** for water, photoabsorption and fluorescence spectra of **poly(SM-2-*co*-MMA)** were measured in acetonitrile containing various concentrations of water (Fig. 6). As with the case of **SM-2**, **poly(SM-2-*co*-MMA)** in absolute acetonitrile exhibited a vibronically-structured photoabsorption band in the range of 300 nm to 400 nm and a feeble and vibronically-structured fluorescence band (λ^{fl}_{max} = *ca.* 420 nm) in the range of 400 nm to 500 nm originating from the anthracene skeleton in the PET active state. The photoabsorption spectra showed unnoticeable changes with the increase in the water content in the acetonitrile solutions. In contrast, the fluorescence intensity of the monomer emission band originating from the anthracene fluorophore increased almost linearly with the increase in the water content in the low water content region below *ca.* 1.0 wt% in the acetonitrile solutions due to the formation of the PET inactive species **poly(SM-2-*co*-MMA)a** by the addition of water molecules (Fig. 1d), while the fluorescence intensity leveled off when the water content reached 1.0 wt% as with the cases of **SM-2** (Fig. 5c). One can see that the acetonitrile solution of **poly(SM-2-*co*-MMA)** without the addition of water did not show any visual fluorescence emission but exhibited the blue fluorescence emission originating from the anthracene fluorophore upon the addition of water (Fig. 3b). Indeed, the plot of the fluorescence peak intensity at around 420 nm *versus* the water fraction in the low water content region below 1.0 wt% showed that the calibration curve had a good linearity with the m_s value of 50, intercept value of 2.61, and R^2 value of 0.994 [F = 50.4[H_2O] + 2.61 (R^2 = 0.994, [H_2O] = 0.0379–0.40 wt%)] (Fig. 5d). However, the m_s value (50) for **poly(SM-2-*co*-MMA)** was much smaller than that (355) of **SM-2** (Table 1). Based on the calibration curve, the DLs and QLs of **poly(SM-2-*co*-MMA)** for water in acetonitrile were estimated to be 0.066 and 0.2 wt%, respectively, which were inferior to those (0.009 and 0.028 wt%) of **SM-2**. The deterioration of the DL and QL values of **poly(SM-2-*co*-MMA)** compared with **SM-2** may be attributed to the dynamic motion of the main chain, to which the anthracene skeleton was directly attached, and hydrophobic environment of the polymer chain, which can inhibit the interaction of the **SM-2** moiety with water molecules, leading to the non-radiative decay of the photoexcited anthracene fluorophore. In fact, in acetonitrile with 1.0 wt% water content, the Φ_{fl} (5%) of **poly(SM-2-*co*-MMA** was lower than that (12%) of **SM-2**. Nevertheless, it was found that the copolymer **poly(SM-2-*co*-MMA)** composed of **SM-2** and MMA can act as a PET-type fluorescent polymeric sensor for the detection and quantification of a trace amount of water in solvents.

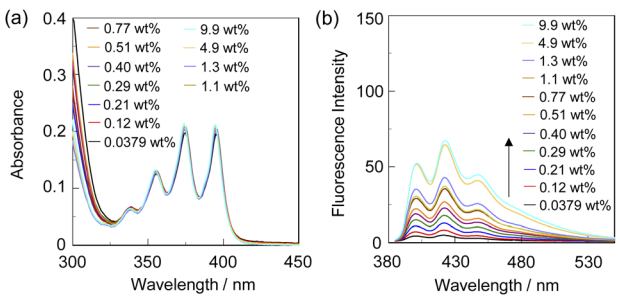

Fig. 6 (a) Photoabsorption and (b) fluorescence spectra (λ^{ex} = 375 nm) of **poly(SM-2-*co*-MMA)** in acetonitrile containing water (0.0379–9.9 wt%). The concentration of the solutions was adjusted so that the absorbance at 375 nm was *ca.* 0.2, that is, the concentration of **SM-2** unit in **poly(SM-2-*co*-MMA)** was *ca.* 2.0 × 10^{-5} M, which was the same as the case of **SM-2** in Fig. 2.

Next, to evaluate the possibility for the PET-type fluorescent sensor to function in polymer matrices for visualization and detection of water, we prepared spin-coated **poly(SM-2-*co*-MMA)** films on glass substrates, and photoabsorption and fluorescence spectra of the spin-coated **poly(SM-2-*co*-MMA)** films before and after exposure to moisture were repeatedly measured several times. In addition, PMMA films doped with **OF-2** or **SM-2** at 15 wt% as well as 50 wt% were prepared on glass substrates by spin-coating process for comparison with the spin-coated **poly(SM-2-*co*-MMA)** films, which contained *ca.* 15 wt% **SM-2** unit (Fig. 7 and 8). The as-prepared 15 wt% and 50 wt% **OF-2**- or **SM-2**-doped PMMA films as well as the **poly(SM-2-*co*-MMA)** films (in dry process) showed a vibronically-structured photoabsorption band in the range of 300 nm to 400 nm originating from the anthracene skeleton (Fig. 7a, c, e and 8a, c). For the corresponding fluorescence spectra in dry process, the 15 wt% **OF-2**- or **SM-2**-doped PMMA films and the **poly(SM-2-*co*-MMA)**

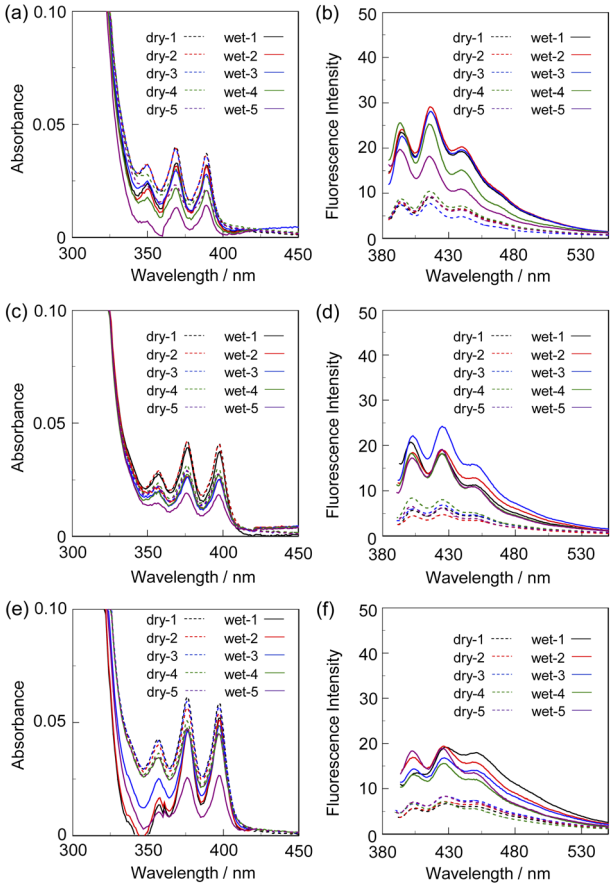

Fig. 7 (a) Photoabsorption and (b) fluorescence spectra (λ^{ex} = 368 nm) of 15 wt% **OF-2**-doped PMMA film before (in dry process) and after (in wet process) exposure to moisture. (c) Photoabsorption and (d) fluorescence spectra (λ^{ex} = 375 nm) of 15 wt% **SM-2**-doped PMMA film before (in dry process) and after (in wet process) exposure to moisture. (e) Photoabsorption and (f) fluorescence spectra (λ^{ex} = 375 nm) of **poly(SM-2-*co*-MMA)** film before (in dry process) and after (in wet process) exposure to moisture. For all the photoabsorption spectra, baseline-correction was made to be the same absorbance at 420 nm.

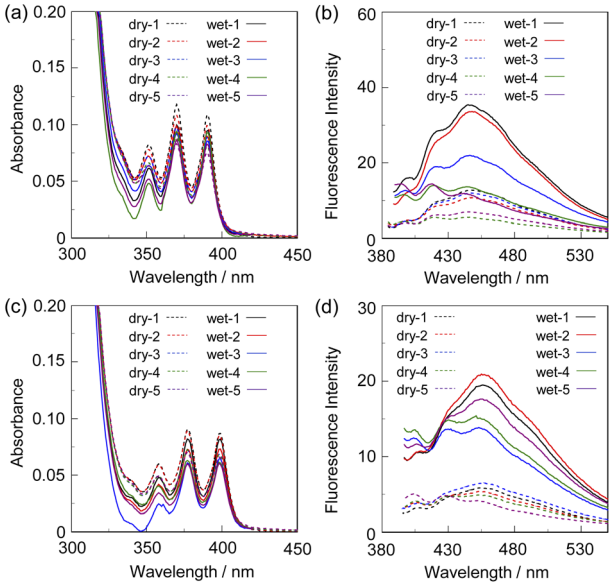

Fig. 8 (a) Photoabsorption and (b) fluorescence spectra (λ^{ex} = 368 nm) of 50 wt% **OF-2**-doped PMMA film before (in dry process) and after (in wet process) exposure to moisture. (c) Photoabsorption and (d) fluorescence spectra (λ^{ex} = 377 nm) of 50 wt% **SM-2**-doped PMMA film before (in dry process) and after (in wet process) exposure to moisture. For all the photoabsorption spectra, baseline-correction was made to be the same absorbance at 420 nm.

films exhibited a feeble and vibronically-structured fluorescence band with a λ^{fl}_{max} at around 415–430 nm in the range of 400 nm to 500 nm, which is attributed to the monomer emission originating from the anthracene fluorophore in the PET active state (Fig. 7b, d and f), but the 50 wt% **OF-2**- or **SM-2**-doped PMMA films showed a broad and feeble fluorescence band with a λ^{fl}_{max} at around 450 nm in the range of 400 nm to 600 nm attributable to the excimer emission originating from the anthracene fluorophore in the PET active aggregate state (Fig. 8b and d). When all the **OF-2**- or **SM-2**-doped PMMA films and the **poly(SM-2-*co*-MMA)** films were exposed to moisture (in wet process), the photoabsorption spectral shape did not undergo appreciable changes, although a slight change in the absorbance was observed due to the disturbance of the baselines in the photoabsorption spectra (Fig. 7a, c, e and 8a, c). For the 15 wt% **OF-2**- or **SM-2**-doped PMMA films and the **poly(SM-2-*co*-MMA)** films, the corresponding fluorescence spectra in wet process showed the enhancement of the vibronically-structured monomer emission band originating from the anthracene fluorophore in the PET inactive state (Fig. 7b, d and f). On the other hand, the 50 wt% **OF-2**- or **SM-2**-doped PMMA films showed an appearance of the monomer emission band with a λ^{fl}_{max} at around 415–430 nm and the enhancement of the excimer emission band with a λ^{fl}_{max} at around 450 nm, that is, the enhancement of the broad fluorescence band originating from the anthracene fluorophore in the range of 400 nm to 600 nm arising from the PET inactive state upon exposure to moisture (Fig. 8b and d). It is worth noting here that when all the **OF-2**- or **SM-2**-doped PMMA films and the **poly(SM-2-*co*-MMA)** films after exposure to moisture were dried in the atmosphere, the photoabsorption and fluorescence spectra recovered the original spectral shapes before exposure to moisture. Actually, one can see that the 15 wt% **SM-2**-doped PMMA films and the **poly(SM-2-*co*-MMA)** films initially exhibited visually imperceptible blue emission in the PET active state but the visual blue monomer emission in the PET inactive state upon exposure to moisture (Fig. 3c and d). Meanwhile, the 50 wt% **SM-2**-doped PMMA films showed feeble green excimer emission in the PET active state before exposure to moisture but the bluish green monomer and excimer emissions in the PET inactive state upon exposure to moisture (Fig. 9f). Therefore, for all the **OF-2**- or **SM-2**-doped PMMA films and the **poly(SM-2-*co*-MMA)** films, the reversibility of the fluorescence intensity at the λ^{fl}_{max} in the dry–wet process was investigated (Fig. 9a–e). It was found that the dry–wet cycles of the 15 wt% **OF-2**- or **SM-2**-doped PMMA films and the **poly(SM-2-*co*-MMA)** films showed a good reversible switching of the fluorescent intensity even in the five times dry–wet process (Fig. 9a–c). However, the 50 wt% **OF-2**- or

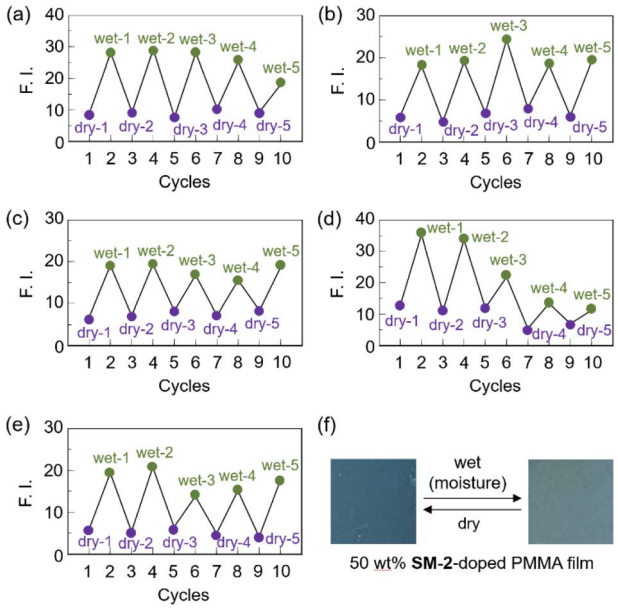

Fig. 9 Reversible switching of fluorescence intensity at around 415–430 nm of (a) 15 wt% OF-2-doped PMMA film, (b) 15 wt% SM-2-doped PMMA film, and (c) poly(SM-2-*co*-MMA) film, and at around 450 nm of (d) 50 wt% OF-2-doped PMMA film and (e) 50 wt% SM-2-doped PMMA film during dry–wet process. (f) Photographs (under 365 nm irradiation) of 50 wt% SM-2-doped PMMA film before and after exposure to moisture.

SM-2-doped PMMA films showed that the fluorescence intensity in the wet process was attenuated from the third time onward (Fig. 9d and e). The poor reversibility of the fluorescence intensity of the 50 wt% **OF-2**- or **SM-2**-doped PMMA films may be attributed to destruction of the films during the dry–wet process and/or promotion of aggregate formation of **OF-2** and **SM-2** after dry process. We also measured the water contact angles on the polymer film surfaces to investigate the hydrophilicity of the 15 wt% **SM-2**-doped PMMA films and the **poly(SM-2-*co*-MMA)** films (Fig. 10). The water contact angles on the polymer film surfaces were 68.3° and 68.2° for the 15 wt% **SM-2**-doped PMMA films and the **poly(SM-2-*co*-MMA)** films, respectively, clearly indicating that the hydrophilicity was similar to each other. Thus, the fact provides the evidence that the both films shows similar reversible switching in the fluorescent intensity in the dry–wet process. Consequently, this work demonstrated that PET-type fluorescent polymer films based on a fluorescence enhancement system produce a satisfactory reversible fluorescence off–on switching between the PET active state and the PET inactive state during the dry–wet process, and thus are one of the most promising and convenient functional dye materials to enable the visualization and detection of moisture and water droplets.

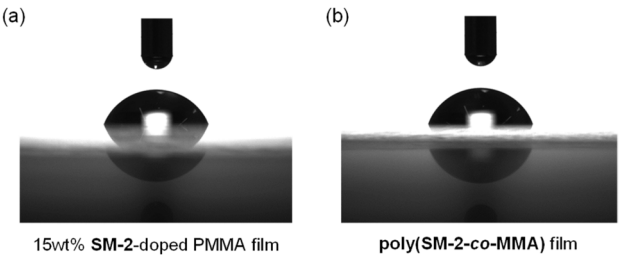

Fig. 10 (a) Water contact angle images of (a) 15 wt% SM-2-doped PMMA film and (b) poly(SM-2-*co*-MMA) film.

Conclusions

We have designed and developed the PET-type fluorescent monomer **SM-2** composed of methyl methacrylate-substituted anthracene fluorophore-AminoMeCNPhenylBPin and the copolymer **poly(SM-2-*co*-MMA)** composed of **SM-2** and MMA, as fluorescent sensors for visualization, detection, and quantification of a trace amount of water. It was found that both **SM-2** and **poly(SM-2-*co*-MMA)** exhibited enhancement of the fluorescence emission with the increase in water content in various solvents (less polar, polar, protic, and aprotic solvents) due to the formation of the PET inactive (fluorescent) species **SM-2a** and **poly(SM-2-*co*-MMA)a**, respectively, by the interaction with water molecules. The detection limit of **poly(SM-2-*co*-MMA)** for water in acetonitrile was 0.066 wt%, indicating that **poly(SM-2-*co*-MMA)** can act as a PET-type fluorescent polymeric sensor for a trace amount of water in solvents, although it was inferior to that (0.009 wt%) of **SM-2**. Moreover, we have achieved the preparation of the spin-coated **poly(SM-2-*co*-MMA)** films as well as 15 wt% **SM-2**-doped PMMA films and demonstrated that both the polymer films produced a satisfactory reversible fluorescence off–on switching between the PET active state under a drying process and the PET inactive state upon exposure to moisture. Consequently, this work proposes that PET-type fluorescent polymer films are one of the most promising and convenient functional dye materials to enable the visualization and detection of moisture and water droplets.

Experimental

General

Melting points were measured with an AS ONE ATM-02. IR spectra were recorded on a SHIMADZU IRTracer-100 spectrometer by the ATR method. ^{1}H and ^{13}C NMR spectra were recorded on a Varian-500 FT NMR spectrometer. High-resolution mass spectral data were acquired by APCI on a Thermo Fisher Scientific LTQ Orbitrap XL. Photoabsorption spectra were observed with a SHIMADZU UV-3600 plus. Fluorescence spectra were measured with a Hitachi F-4500 spectrophotometer. The fluorescence quantum yields were determined by a Hamamatsu C9920-01 equipped with a CCD using a calibrated integrating sphere system. The addition of water to 1,4-dioxane, THF, acetonitrile, or ethanol solutions containing **SM-2** or acetonitrile solutions containing **poly(SM-2-*co*-MMA)** was made in terms of weight percent (wt%). The determination of water in solvents was done with MKC-610 and MKA-610 Karl Fischer moisture titrators (Kyoto Electronics Manufacturing Co., Ltd) based on Karl Fischer coulometric titration for below 1.0 wt% and volumetric titration for 1.0–10 wt%. Polymer number-average molecular weights (M_n) and

molecular weight distributions (M_w/M_n) were determined by size exclusion chromatography (SEC) at 40 °C using a SHIMADZU Prominence-i LC-2030 plus with a guard column (LF-G, Shodex), two series-connected columns (LF-804, Shodex), a UV detector, and a differential refractive index detector (RID-20A). THF was used as the eluent, and poly(methyl methacrylate) (PMMA) standards were used to calibrate the SEC system. Static water contact angles were measured at five different positions on a substrate by the sessile drop technique using a Kyowa Interface Science DMo-602 contact angle meter.

Synthesis

(10-(((5-Cyano-2-(4,4,5,5-tetramethyl-1,3,2-dioxaborolan-2-yl) benzyl)(methyl)amino)methyl)anthracen-9-yl)methyl methacrylate (SM-2). A solution of **SM-1** (0.100 g, 0.203 mmol), 4-dimethylaminopyridine (0.003 g, 0.025 mmol), and triethylamine (0.17 mL, 1.21 mmol) in dry THF (15 mL) was stirred for 0.5 h at 0 °C under nitrogen atmosphere, and then, methacryloyl chloride was added slowly to the solution. After stirring for 18 h at room temperature, the reaction mixture was concentrated. The residue was chromatographed on alumina (methanol : dichloromethane = 1 : 100 as eluent) to give **SM-2** (0.064 g, yield 56%) as a light yellow solid; m.p. 137–139 °C; FT-IR (ATR): $\tilde{\nu}$ = 2978, 2230, 1713, 1449, 1344, 1315, 1271, 1142 cm^{-1}; ^1H NMR (500 MHz, acetone-d_6): 1.29 (s, 12H), 1.87 (s, 3H), 2.32 (s, 3H), 4.04 (s, 2H), 4.51 (s, 2H), 5.56 (s, 1H), 5.97 (s, 1H), 6.24 (s, 2H), 7.50–7.64 (m, 5H), 7.73 (s, 1H), 7.87 (d, J = 7.5 Hz, 1H), 8.46 (d, J = 8.7 Hz, 2H), 8.51 (d, J = 8.8 Hz, 2H) ppm; ^{13}C NMR (125 MHz, $CDCl_3$): δ = 18.49, 25.13, 42.97, 52.68, 59.45, 60.81, 84.11, 113.64, 119.18, 124.66, 125.54, 125.79, 126.18, 127.21, 129.70, 130.88, 131.28, 132.02, 132.16, 135.57, 136.24, 146.43, 167.72 ppm (two aromatic carbon signals were not observed owing to overlapping resonances); HRMS (APCI): m/z (%): [$M^{+\bullet}$] calcd for $C_{35}H_{37}N_2O_4B$, 560.28409; found 560.28491.

Preparation of poly(SM-2-*co*-MMA)

A solution of **SM-2** (0.023 g, 0.042 mmol), methyl methacrylate (0.100 mL, 0.949 mmol), and azobis(isobutyronitrile) (0.811 mg, 0.005 mmol) in toluene (0.77 mL) was degassed with four freeze–pump–thaw cycles, and then, the solution was stirred for 18 h at 70 °C under nitrogen atmosphere. The reaction mixture was concentrated, and the resulting residue was dissolved in dichloromethane. The dichloromethane solution was poured into *n*-hexane and the resulting precipitate was collected to give **poly(SM-2-*co*-MMA)** (0.020 g, yield 17%) as a white solid; m.p. 160–200 °C; FT-IR (ATR): $\tilde{\nu}$ = 2991, 2949, 2231, 1728, 1481, 1449, 1387, 1348, 1267, 1240, 1190, 1146 cm^{-1}; ^1H NMR (500 MHz, $CDCl_3$): 0.82 (br, C–CH_3 for MMA), 0.82 (br, C–CH_3 for MMA in **SM-2** unit), 1.31 (s, C$\underline{H}_3$ for BPin), 1.81 (br, C$\underline{H}_2$ for MMA and MMA in **SM-2** unit), 2.30 (s, N–CH_3 for **SM-2** unit), 3.60 (br, O–CH_3 for MMA), 3.96 (s, N–CH_2-Ph for **SM-2** unit), 4.50 (s, N–CH_2–An for **SM-2** unit), 6.05 (br, O–CH_2–An for **SM-2** unit), 7.45–7.60 (m, 4C$\underline{H}$ at 2,3,6,7-positions on An and C$\underline{H}$ at 6-position on Ph for **SM-2** unit), 7.63 (br, C$\underline{H}$ at 4- position on Ph for **SM-2** unit), 7.83 (br, C$\underline{H}$ at 3- position on Ph for **SM-2** unit), 8.23–8.40 (m, 4C$\underline{H}$ at 1,4,5,8-positions on An for **SM-2** unit) ppm, the molar ratio (y/x) of MMA unit (y) and **SM-2** unit (x) and the weight percentage (wt%) of **SM-2** in the obtained **poly(SM-2-*co*-MMA)** was determined to be *ca.* 40 and *ca.* 15 wt%, respectively, from the ^1H NMR spectrum; SEC M_n = 18 900, M_w/M_n = 2.08; UV-Vis λ^{abs} = 339, 356, 375, 395 nm, PL λ^{fl} = 401, 422, 447, 480 nm (in acetonitrile).

Preparation of poly(SM-2-*co*-MMA) film

A solution of **poly(SM-2-*co*-MMA)** (8.0 mg) in toluene (0.4 mL) was stirred for 3 h at room temperature, while **poly(SM-2-*co*-MMA)** has dissolved quickly. To prepare a polymer film, 150 μL of a **poly(SM-2-*co*-MMA)** solution was spin-coated (1000 rpm for 30 s) on a glass substrate (MIKASA MS-A-100 Opticoat Spincoater). The spin-coated films were dried in air. The resulting **poly(SM-2-*co*-MMA)** films were exposed to moisture for 60 s using a humidifier.

Preparation of 15 wt% and 50 wt% OF-2- or SM-2-doped PMMA films

A solution of PMMA (8.5 mg and 5.0 mg for 15 wt% and 50 wt%, respectively) in toluene (0.5 mL) was stirred for several hours at 60–70 °C until PMMA has dissolved, and then, **OF-2** or **SM-2** (1.5 mg and 5.0 mg for 15 wt% and 50 wt%, respectively) was added to the solution. To prepare a polymer film, 150 μL of a **OF-2**-PMMA solution or a **SM-2**-PMMA solution was spin-coated (1000 rpm for 30 s) on a glass substrate (MIKASA MS-A-100 Opticoat Spincoater). The spin-coated films were dried in air. The resulting 15 wt% and 50 wt% **OF-2**- or **SM-2**-doped PMMA films were exposed to moisture for 60 s using a humidifier.

Conflicts of interest

There are no conflicts to declare.

Acknowledgements

This work was supported by Grants-in-Aid for Scientific Research (B) from the Japan Society for the Promotion of Science (JSPS) KAKENHI Grant Number 19H02754 and 22H02123, JST Adaptable and Seamless Technology Transfer Program through Target-driven R&D (A-STEP) Grant Number JPMJTM20RB, and Ogasawara Toshiaki Memorial Foundation.

Notes and references

1 H. S. Jung, P. Verwilst, W. Y. Kim and J. S. Kim, Fluorescent and colorimetric sensors for the detection of humidity or water content, *Chem. Soc. Rev.*, 2016, **45**, 1242–1256.

2 F. Wu, L. Wang, H. Tang and D. Cao, Excited State Intramolecular Proton Transfer Plus Aggregation-Induced Emission-Based Diketopyrrolopyrrole Luminogen: Photophysical Properties and Simultaneously Discriminative Detection of Trace Water in Three Organic Solvents, *Anal. Chem.*, 2019, **91**, 5261–5269.

3 W. Cheng, Y. Xie, Z. Yang, Y. Sun, M.-Z. Zhang, Y. Ding and W. Zhang, General Strategy for in Situ Generation of a Coumarin-Cu^{2+} Complex for Fluorescent Water Sensing, *Anal. Chem.*, 2019, **91**, 5817–5823.

4 S. Song, Y. Zhang, Y. Yang, C. Wang, Y. Zhou, C. Zhang, Y. Zhao, M. Yang and Q. Lin, Ratiometric fluorescence detection of trace water in organic solvents based on aggregation-induced emission enhanced Cu nanoclusters, *Analyst*, 2018, **143**, 3068–3074.

5 L. Liu, Q. Zhang, H. Duan, C. Li and Y. Lu, An ethanethioate functionalized polythiophene as an optical probe for sensitive and fast detection of water content in organic solvents, *Anal. Methods*, 2021, **13**, 3792–3798.

6 T. Maeda and F. Würthner, Halochromic and hydrochromic squaric acid functionalized perylene bisimide, *Chem. Commun.*, 2015, **51**, 7661–7664.

7 D. Wang, H. Zhao, H. Li, S. Sun and Y. Xu, A fluorescent "glue" of water triggered by hydrogen-bonding cross-linking, *J. Mater. Chem. C*, 2016, **4**, 11050–11054.

8 S. Roy, S. Das, A. Ray and P. P. Parui, An inquisitive fluorescence method for the real-time detection of trace moisture in polar aprotic solvents with the application of water rancidity in foodstuffs, *New J. Chem.*, 2021, **45**, 4574–4583.

9 S. Mishra and A. K. Singh, Optical sensors for water and humidity and their further applications, *Coord. Chem. Rev.*, 2021, **445**, 214063.

10 J. Othong, J. Boonmak, F. Kielar and S. Youngme, Dual Function Based on Switchable Colorimetric Luminescence for Water and Temperature Sensing in Two-Dimensional Metal–Organic Framework Nanosheets, *ACS Appl. Mater. Interfaces*, 2020, **12**, 41776–41784.

11 Y. Zhou, G. Baryshnikov, X. Li, M. Zhu, H. Ågren and L. Zhu, Anti-Kasha's Rule Emissive Switching Induced by Intermolecular H-Bonding, *Chem. Mater.*, 2018, **30**, 8008–8016.

12 P. Kumar, R. Sakla, A. Ghosh and D. A. Jose, Reversible Colorimetric Sensor for Moisture Detection in Organic Solvents and Application in Inkless Writing, *ACS Appl. Mater. Interfaces*, 2017, **9**, 25600–25605.

13 H. Yan, S. Guo, F. Wu, P. Yu, H. Liu, Y. Li and L. Mao, Carbon Atom Hybridization Matters: Ultrafast Humidity Response of Graphdiyne Oxides, *Angew. Chem., Int. Ed.*, 2018, **57**, 3922–3926.

14 K. Tanaka, K. Nishino, S. Ito, H. Yamane, K. Suenaga, K. Hashimoto and Y. Chujo, Development of solid-state emissive o-carboranes and theoretical investigation of the mechanism of the aggregation-induced emission behaviors of organoboron "element-blocks", *Faraday Discuss.*, 2017, **196**, 31–42.

15 H. Mori, K. Nishino, K. Wada, Y. Morisaki, K. Tanaka and Y. Chujo, Modulation of luminescence chromic behaviors and environment-responsive intensity changes by substituents in bis-*o*-carborane-substituted conjugated molecules, *Mater. Chem. Front.*, 2018, **2**, 573–579.

16 K. Nishino, H. Yamamoto, J. Ochi, K. Tanaka and Y. Chujo, Time-Dependent Emission Enhancement of the Ethynylpyrene-o-Carborane Dyad and Its Application as a Luminescent Color Sensor for Evaluating Water Contents in Organic Solvents, *Chem.–Asian J.*, 2019, **14**, 1577–1581.

17 Y.-C. Liu, G.-D. Lu, J.-H. Zhou, J.-W. Rong, H.-Y. Liu and H.-Y. Wang, Fluoranthene dyes for the detection of water content in methanol, *RSC Adv.*, 2022, **12**, 7405–7412.

18 W.-E. Lee, Y.-J. Jin, L.-S. Park and G. Kwak, Fluorescent Actuator Based on Microporous Conjugated Polymer with Intramolecular Stack Structure, *Adv. Mater.*, 2012, **24**, 5604–5609.

19 D.-C. Han, Y.-J. Jin, J.-H. Lee, S.-I. Kim, H.-J. Kim, K.-H. Song and G. Kwak, Environment-Specific Fluorescence Response of Microporous, Conformation-Variable Conjugated Polymer Film to Water in Organic Solvents: On-line Real-Time Monitoring in Fluidic Channels, *Macromol. Chem. Phys.*, 2014, **215**, 1068–1076.

20 Q. Deng, Y. Li, J. Wu, Y. Liu, G. Fang, S. Wang and Y. Zhang, Highly sensitive fluorescent sensing for water based on poly(*m*-aminobenzoic acid), *Chem. Commun.*, 2012, **48**, 3009–3011.

21 J. Lee, M. Pyo, S. Lee, J. Kim, M. Ra, W.-Y. Kim, B. J. Park, C. W. Lee and J.-M. Kim, Hydrochromic conjugated polymers for human sweat pore mapping, *Nat. Commun.*, 2014, **5**, 3736.

22 T. Fumoto, S. Miho, Y. Mise, K. Imato and Y. Ooyama, Polymer films doped with fluorescent sensor for moisture and water droplet based on photo-induced electron transfer, *RSC Adv.*, 2021, **11**, 17046–17050.

23 S. Miho, T. Fumoto, Y. Mise, K. Imato, S. Akiyama, M. Ishida and Y. Ooyama, Development of highly sensitive fluorescent sensor and fluorescent sensor-doped polymer films for trace amounts of water based on photo-induced electron transfer, *Mater. Adv.*, 2021, **2**, 7662–7670.

24 I. M. Resta and F. Galindo, Phenol-based styrylpyrylium dyes for trace water detection via chromogenic and fluorogenic responses, *Dyes Pigm.*, 2022, **197**, 109908.

25 Z. Li, Q. Yang, R. Chang, G. Ma, M. Chen and W. Zhang, *N*-Heteroaryl-1,8-naphthalimide fluorescent sensor for water: Molecular design, synthesis and properties, *Dyes Pigm.*, 2011, **88**, 307–314.

26 W. Chen, Z. Zhang, X. Li, H. Ågren and J. Su, Highly sensitive detection of low-level water content in organic solvents and cyanide in aqueous media using novel solvatochromic AIEE fluorophores, *RSC Adv.*, 2015, **5**, 12191–12201.

27 S. Tsumura, T. Enoki and Y. Ooyama, A colorimetric and fluorescent sensor for water in acetonitrile based on intramolecular charge transfer: D–$(\pi$–A$)_2$-type pyridine–boron trifluoride complex, *Chem. Commun.*, 2018, **54**, 10144–10147.

28 T. Enoki and Y. Ooyama, Colorimetric and ratiometric fluorescence sensing of water based on 9-methyl pyrido [3,4-*b*]indole-boron trifluoride complex, *Dalton Trans.*, 2019, **48**, 2086–2092.

29 K. Imato, T. Enoki and Y. Ooyama, Development of an intramolecular charge transfer-type colorimetric and fluorescence sensor for water by fusion with a juloidine structure and complexation with boron trifluoride, *RSC Adv.*, 2019, **9**, 31466–31473.

30 S. Tusmura, K. Ohira, K. Imato and Y. Ooyama, Development of optical sensor for water in acetonitrile based on propeller-structured BODIPY-type pyridine–boron trifluoride complex, *RSC Adv.*, 2020, **10**, 33836–33843.

31 C.-G. Niu, P.-Z. Qin, G.-M. Zeng, X.-Q. Gui and A.-L. Guan, Fluorescence sensor for water in organic solvents prepared from covalent immobilization of 4-morpholinyl-1, 8-naphthalimide, *Anal. Bioanal. Chem.*, 2007, **387**, 1067–1074.

32 Z.-Z. Li, C.-G. Niu, G.-M. Zeng and P.-Z. Qin, Fluorescence Sensor for Water Content in Organic Solvents Based on Covalent Immobilization of Benzothioxanthene, *Chem. Lett.*, 2009, **38**, 698–699.

33 D. Citterio, K. Minamihashi, Y. Kuniyoshi, H. Hisamoto, S. Sasaki and K. Suzuki, Optical determination of low-level water concentrations in organic solvents using fluorescent acridinyl dyes and dye-immobilized polymer membranes, *Anal. Chem.*, 2001, **73**, 5339–5345.

34 C.-G. Niu, A.-L. Guan, G.-M. Zeng, Y.-G. Liu and Z.-W. Li, Fluorescence water sensor based on covalent immobilization of chalcone derivative, *Anal. Chim. Acta*, 2006, **577**, 264–270.

35 W. Liu, Y. Wang, W. Jin, G. Shen and R. Yu, Solvatochromogenic flavone dyes for the detection of water in acetone, *Anal. Chim. Acta*, 1999, **383**, 299–307.

36 J. S. Kim, M. G. Choi, Y. Huh, M. H. Kim, S. H. Kim, S. Y. Wang and S.-K. Chang, Determination of Water Content in Aprotic Organic Solvents Using 8-Hydroxyquinoline Based Fluorescent Probe, *Bull. Korean Chem. Soc.*, 2006, **27**, 2058–2060.

37 H. Mishra, V. Misra, M. S. Mehata, T. C. Pant and H. B. Tripathi, Fluorescence Studies of Salicylic Acid Doped Poly(vinyl alcohol) Film as a Water/Humidity Sensor, *J. Phys. Chem. A*, 2004, **108**, 2346–2352.

38 A. C. Kumar and A. K. Mishra, 1-Naphthol as an excited state proton transfer fluorescent probe for sensing bound-water hydration of polyvinyl alcohol, *Talanta*, 2007, **71**, 2003–2006.

39 Y. Ooyama, M. Sumomogi, T. Nagano, K. Kushimoto, K. Komaguchi, I. Imae and Y. Harima, Detection of water in organic solvents by photo-induced electron transfer method, *Org. Biomol. Chem.*, 2011, **9**, 1314–1316.

40 Y. Ooyama, A. Matsugasako, K. Oka, T. Nagano, M. Sumomogi, K. Komaguchi, I. Imae and Y. Harima, Fluorescence PET (photo-induced electron transfer) sensors for water based on anthracene–boronic acid ester, *Chem. Commun.*, 2011, **47**, 4448–4450.

41 Y. Ooyama, A. Matsugasako, Y. Hagiwara, J. Ohshita and Y. Harima, Highly sensitive fluorescence PET (photo-induced electron transfer) sensor for water based on anthracene–bisboronic acid ester, *RSC Adv.*, 2012, **2**, 7666–7668.

42 Y. Ooyama, K. Furue, K. Uenaka and J. Ohshita, Development of highly-sensitive fluorescence PET (photo-induced electron transfer) sensor for water: anthracene–boronic acid ester, *RSC Adv.*, 2014, **4**, 25330–25333.

43 Y. Ooyama, M. Hato, T. Enoki, S. Aoyama, K. Furue, N. Tsunoji and J. Ohshita, A BODIPY sensor for water based on a photo-induced electron transfer method with fluorescence enhancement and attenuation systems, *New J. Chem.*, 2016, **40**, 7278–7281.

44 Y. Ooyama, R. Sagisaka, T. Enoki, N. Tsunoji and J. Ohshita, Tetraphenylethene– and diphenyldibenzofulvene–anthracene-based fluorescence sensors possessing photo-induced electron transfer and aggregation-induced emission enhancement characteristics for detection of water, *New J. Chem.*, 2018, **42**, 13339–13350.

45 D. Jinbo, K. Imato and Y. Ooyama, Fluorescent sensor for water based on photo-induced electron transfer and Förster resonance energy transfer: anthracene-(aminomethyl)phenylboronic acid ester-BODIPY structure, *RSC Adv.*, 2019, **9**, 15335–15340.

46 D. Jinbo, K. Ohira, K. Imato and Y. Ooyama, Development of fluorescent sensors based on a combination of PET (photo-induced electron transfer) and FRET (Förster resonance energy transfer) for detection of water, *Mater. Adv.*, 2020, **1**, 354–362.

47 L. Ding, Z. Zhang, X. Li and J. Su, Highly sensitive determination of low-level water content in organic solvents using novel solvatochromic dyes based on thioxanthone, *Chem. Commun.*, 2013, **49**, 7319–7321.

48 Y. Zhang, D. Li, Y. Li and J. Yu, Solvatochromic AIE luminogens as supersensitive water detectors in organic solvents and highly efficient cyanide chemosensors in water, *Chem. Sci.*, 2014, **5**, 2710–2716.

49 Y. Mise, K. Imato, T. Ogi, N. Tsunoji and Y. Ooyama, Fluorescence sensors for detection of water based on tetraphenylethene–anthracene possessing both solvatofluorochromic properties and aggregation-induced emission (AIE) characteristics, *New J. Chem.*, 2021, **45**, 4164–4173.

50 N. Zhao, Z. Yang, J. W. Y. Lam, H. H. Y. Sung, N. Xie, S. Chen, H. Su, M. Gao, I. D. Williams, K. S. Wong and B. Z. Tang, Benzothiazolium-functionalized tetraphenylethene: an AIE luminogen with tunable solid-state emission, *Chem. Commun.*, 2012, **48**, 8637–8639.

51 X. Y. Shen, Y. J. Wang, H. Zhang, A. Qin, J. Z. Sun and B. Z. Tang, Conjugates of tetraphenylethene and diketopyrrolopyrrole: tuning the emission properties with phenyl bridges, *Chem. Commun.*, 2014, **50**, 8747–8750.

52 F. Khan, A. Ekbote, S. M. Mobin and R. Misra, Mechanochromism and Aggregation-Induced Emission in Phenanthroimidazole Derivatives: Role of Positional Change of Different Donors in a Multichromophoric Assembly, *J. Org. Chem.*, 2021, **86**, 1560–1574.

53 Q. Wu, H. Xiong, Y. Zhu, X. Ren, L.-L. Chu, Y.-F. Yao, G. Huang and J. Wu, Self-Healing Amorphous Polymers with Room-Temperature Phosphorescence Enabled by Boron-Based Dative Bonds, *ACS Appl. Polym. Mater.*, 2020, **2**, 699–705.

54 W. Wu, N. Shi, J. Zhang, X. Wu, T. Wang, L. Yang, R. Yang, C. Ou, W. Xue, X. Feng, L. Xie and W. Huang, Electrospun fluorescent sensors for the selective detection of nitro explosive vapors and trace water, *J. Mater. Chem. A*, 2018, **6**, 18543–18550.

55 W. Wang, S. Gao and B. Wang, Building Fluorescent Sensors by Template Polymerization: The Preparation of a Fluorescent Sensor for d-Fructose, *Org. Lett.*, 1999, **1**, 1209–1212.